学位論文

Critical role of Myc activation in mouse hepatocarcinogenesis induced by the activation of AKT and RAS pathways

（AKT および RAS 経路活性化によるマウス肝発癌過程における
Myc 遺伝子活性化の役割）

旭川医科大学大学院医学系研究科博士課程医学専攻
辛　　冰

（山本 雅大，藤井 清永，大塩 貴子，陳 錫，岡田 陽子，
渡邉 賢二，三代川 斉之，古川 博之，西川 祐司）

Critical role of Myc activation in mouse hepatocarcinogenesis induced by the activation of AKT and RAS pathways

Bing Xin[1], Masahiro Yamamoto[1], Kiyonaga Fujii[1], Takako Ooshio[1], Xi Chen[1], Yoko Okada[1], Kenji Watanabe[1,3], Naoyuki Miyokawa[2], Hiroyuki Furukawa[3], and Yuji Nishikawa[1]

[1]Division of Tumor Pathology, Department of Pathology, Asahikawa Medical University, Asahikawa, Hokkaido 078-8510, Japan

[2]Department of Surgical Pathology, Asahikawa Medical University Hospital, Asahikawa, Hokkaido 078-8510, Japan

[3]Division of Gastroenterological and General Surgery, Department of Surgery, Asahikawa Medical University, Asahikawa, Hokkaido 078-8510, Japan

Corresponding author: Yuji Nishikawa, M.D., Ph.D., Division of Tumor Pathology, Department of Pathology, Asahikawa Medical University, Higashi 2-1-1-1, Midorigaoka, Asahikawa, Hokkaido 078-8510, Japan. Tel: +81-166-68-2370; Fax: +81-166-68-2379. E-mail: nishikwa@asahikawa-med.ac.jp

Running head: Spontaneous and forced Myc activation in mouse hepatocarcinogenesis

Word count: 4554 (excluding Figure Legends)

Number of figures: 8; **number of tables:** 0

Number of supplementary figures: 8; **number of supplementary tables:** 6

Keywords: hepatocellular carcinoma, oncogenes, transposon-mediated gene transfer, proliferation, apoptosis

ABSTRACT

MYC activation at modest levels has been frequently found in hepatocellular carcinoma (HCC). However, its significance in hepatocarcinogenesis has remained obscure. Here we examined the roles of Myc activation in mouse liver tumors induced by hepatocytic expression of myristoylated *AKT* (*AKT*) and/or mutant $HRAS^{V12}$ (*HRAS*) via transposon-mediated gene integration. *AKT* or *HRAS* alone required 5 months to induce liver tumors, whereas their combination generated HCC within 8 weeks. Cointroduction of *AKT* and *HRAS* induced lipid-laden preneoplastic cells that grew into nodules composed of tumor cells with or without intracytoplasmic lipid, with the latter being more proliferative and associated with spontaneous Myc expression. *AKT*/*HRAS*–induced tumorigenesis was almost completely abolished when MadMyc, a competitive Myc inhibitor, was expressed simultaneously. The Tet-On induction of MadMyc in preneoplastic cells significantly inhibited the progression of *AKT/HRAS*-induced tumors; its induction in transformed cells suppressed their proliferative activity with alterations in lipid metabolism and protein translation. Transposon-mediated Myc overexpression facilitated tumorigenesis by *AKT* or *HRAS*, and when it was cointroduced with *AKT* and *HRAS*, diffusely infiltrating tumors without lipid accumulation developed as early as two weeks. Examination of the dose-responses of *Myc* in the enhancement of *AKT/HRAS*-induced tumorigenesis revealed that a reduction to one-third retained enhancing effect but three-times greater introduction damped the process with increased apoptosis. Myc overexpression suppressed the mRNA expression of proteins involved in the synthesis of fatty acids, and when combined with *HRAS* introduction, it also suppressed the mRNA expression of proteins involved in their degradation. Finally, the MYC-positive human HCC was characterized by the cytoplasm devoid of lipid accumulation, prominent nucleoli, and a higher proliferative activity. Our results demonstrate that in hepatocarcinogenesis induced by both activated

AKT and HRAS, activation of endogenous Myc is an enhancing factor and adequate levels of Myc deregulation further facilitate the process with alterations in cellular metabolism.

INTRODUCTION

As a prototypic oncogene, *MYC* actively participates in the development of various human cancers, including hepatocellular carcinoma (HCC).[1, 2] Although a significant copy number gain of 8q24 containing *MYC* has been reported to be positive in a relatively small fraction (4-24%) of HCC cases,[3] modest multiplication (2- to 6-fold) has been found in up to 44% of cases.[4] *MYC* gene expression is known to be increased due to hypomethylation of its promoter early in hepatocarcinogenesis.[5] Furthermore, the *MYC* (or a mouse ortholog *Myc*) gene product, MYC (or mouse Myc), could be posttranslationally modified and its stability is increased through its cooperation with activated PI3K and RAS-mitogen activated protein kinase (MAPK) pathways.[6]

MYC has been shown to contribute to cell proliferation and tumorigenesis in various ways.[7] It directly affect the cell cycle machinery by increasing the expression of E2F, as well as cyclin D and cyclin-dependent kinase (CDK) 4, which then activate cyclin E and CDK2 via sequestration of p27.[8] MYC is involved in transcriptional elongation of many genes with E-boxes in their promoter.[1] MYC also affects posttranscriptional gene expression mechanisms via positive feedback activation of an eukaryotic translation initiation factor (eIF4E)[9] and ribosome biogenesis by regulating RNA polymerases I, II, and III.[10] Furthermore, prior to G1-S transition, MYC induces metabolic reprogramming, involving glycolysis and glutaminolysis, which is necessary for efficient cell proliferation.[1, 2] Using liver-specific transgenic mouse systems with the albumin enhancer/promoter, deregulated MYC expression has been demonstrated to induce liver tumors, with synergistic interactions with mutant Hras[11] or overexpression of E2F1 or transforming growth factor-α.[12] However, there has been a new confounding report showing that liver-specific overexpression of MYC does not promote hepatocarcinogenesis triggered by

conditional expression of mutant Hras.[13] Thus, at present, the precise roles of deregulated Myc expression in hepatocarcinogenesis have not yet been clarified.

By combining the Sleeping Beauty (SB) transposon system[14] and hydrodynamic tail vein injection,[15] long-term *in vivo* expression of exogenous genes in mouse hepatocytes is possible,[16] and the introduction of various oncogenes has generated liver cancers.[17] Recently, the transposon-mediated gene integration of both activated (myristoylated) *AKT* (*myrAKT*) and mutant *NRAS* (*NRAS*^{V12}) has been shown to induce multiple HCC in as little as one month,[18] contrasting with the time course of tumorigenesis induced by *myrAKT* alone, which usually takes several months.[19] Interestingly, a spontaneous increase of Myc has been demonstrated during the tumorigenic process.[18] Although it has been shown that MYC induces liver tumors with the appearance of cancer stem-like chemoresistant cells,[20] the interaction of MYC with other oncogenic pathways has not been examined.

In this study, we explored the effects of spontaneous expression and forced overexpression of Myc on tumorigenesis by transposon-mediated activation of phosphatidylinositol 3-kinase (PI3K) and/or RAS-MAPK pathways. Our results show that both activation of endogenous Myc and deregulated Myc expression significantly contribute to hepatocarcinogenesis.

RESULTS

Introduction of activated *AKT* or mutant *HRAS* into hepatocytes induces hepatocellular carcinoma after long periods of incubation.

Hydrodynamic tail vein injection (HTVi)-mediated introduction of either *myrAKT* (*AKT* henceforward) or mutant *HRAS* (*HRAS* henceforward) alone induced multiple tumors after 20-28 weeks (Fig. 1a). Kang

et al.[21] reported that similar introduction of mutant *NRAS* (*NRAS*^{G12V}) did not induce liver tumors due to oncogene-induced senescence with immune response. However, in our experiments using mutant *HRAS*, even at 5 weeks after HTVi, numerous transduced hepatocytes were present and invoked only focal and limited immune reaction (Supplementary Fig. 1a). Furthermore, these transduced hepatocytes and subsequent tumor cells did not express senescence markers (p16 and p21) (Supplementary Fig. 1b, c). Although the reasons for this discrepancy are unclear, it might reflect functional differences between these RAS isoforms.[22, 23]

The tumors induced by either oncogenes showed histological features of HCC (Fig. 1b). However, *AKT*-induced tumors demonstrated more marked lipid accumulation than *HRAS*-induced tumors, which was confirmed to be triglyceride by Sudan III staining (Fig. 1b). Immunohistochemical studies revealed the highly phosphorylated status of AKT in *AKT*-induced tumors but not in *HRAS*-induced tumors (Fig. 1c). In contrast, the presence of highly phosphorylated ERK in the nucleus and cytoplasm was demonstrated in *HRAS*-induced tumors, whereas there was weak and heterogeneous phosphorylation of ERK in *AKT*-induced tumors (Fig. 1c). Myc immunohistochemistry with tyramide signal amplification (TSA) did not detect Myc activation in either tumors (Fig. 1c).

Activation of both AKT and HRAS facilitates hepatocarcinogenesis with decreased lipid accumulation and Myc activation.

Following the concomitant introduction of *AKT* and *HRAS*, multiple large tumors appeared as early as 8 weeks (Fig. 2a). Microscopically, preneoplastic hepatocytes with lipid accumulation were readily detected after 2 weeks and they grew into HCC composed of tumor cells with or without intracytoplasmic lipid accumulation (Fig. 2b). Ki-67 immunohistochemistry revealed that the tumors induced by *AKT* and *HRAS* (*AKT/HRAS*) were more proliferative than those induced by *AKT* or *HRAS*

alone (Fig. 2c, d). In the *AKT/HRAS*-induced tumors, tumor cells without discernible lipid accumulation showed higher proliferative activity than those with abundant lipid (Fig. 2e). Although the preneoplastic cells observed after 2 weeks of injection were negative for Myc, some tumor cells observed after 8 weeks showed weak nuclear Myc expression (Fig. 2f). Myc-positive tumor cells were more frequently found in cells without lipid accumulation (Fig. 2g). Double immunohistochemistry confirmed that Myc-positive tumor cells were more frequently positive for Ki-67 (Fig. 2h, i). The expression of Myc was not accompanied with an increase of its mRNA (Supplementary Fig. 3).

Myc inhibition by MadMyc suppressed hepatocarcinogenesis induced by concomitant introduction of *AKT* and *HRAS*

To examine the significance of the activation of endogenous Myc in *AKT*/*HRAS*-induced tumors, we concomitantly introduced *MadMyc*, which inhibits Myc activity in a dominant-negative manner.[24, 25] MadMyc introduction almost completely abolished *AKT/HRAS*-induced tumorigenesis (Fig. 3a). There were only scattered swollen hepatocytes with lipid accumulation in the liver in which *MadMyc* was introduced (Fig. 3b). All the *AKT/HRAS*-induced tumor cells, as well as the swollen hepatocytes in the *AKT/HRAS/MadMyc*-treated liver were positive for HA, which was tagged to both AKT and MadMyc, indicating that they were transduced cells (Fig. 3b). Quantitative analysis of HA-positive area demonstrated that MadMyc dramatically inhibited *AKT/HRAS*-induced hepatocarcinogenesis (Fig. 3c).

Next we examined the effect of MadMyc on progression of *AKT/HRAS*-induced preneoplastic hepatocytes. MadMyc was induced by doxycycline (Dox) using the Tet-On system two weeks following the introduction of the plasmids, when only preneoplastic hepatocytes were present. The induction of MadMyc significantly suppressed the enlargement of the liver at 4 weeks (Fig. 3d, Supplementary Fig. 2a). Microscopically, in contrast to multiple coalescent tumor nodules in the Dox (-) control, there were

scattered large cells with lipid accumulation in the livers of Dox-treated mice (Fig. 3e). These cells were positive for both HA and phosphorylated AKT, although the staining intensity of the lipid-rich cells were relatively low (Fig. 3e). Dox treatment greatly reduced the area containing HA-positive transduced cells (Fig. 3f). HA-positive cells in Dox-treated animals tended to be more abundant in cytoplasmic lipid (Fig. 3g) and less proliferative (Fig. 3e, h) as compared with those in the Dox (-) control. No significant apoptotic cell death was induced by Dox treatment (Supplementary Fig. 4). In another set of experiments, whereas most of the Dox (-) control mice were dead or severely ill due to massive liver tumors within 7 weeks, all of Dox-treated mice survived and appeared well (Supplementary Fig. 5a, b). The tumors in Dox-treated mice were smaller in number and size and mainly composed of cells with marked lipid accumulation (Supplementary Fig. 5c).

We also explored whether MadMyc suppressed the proliferation of neoplastic hepatocytes by the induction of MadMyc 4 weeks after the introduction of *AKT* and *HRAS*, when incipient tumor nodules emerged. Although Dox treatment for 2 weeks did not affect the liver weight (Fig. 4a, Supplementary Fig. 3b), it induced lipid accumulation in tumor cells (Fig. 4b). This was associated with the suppression of proliferative activity (Fig. 4b, c). The induction of *MadMyc* mRNA by Dox treatment was confirmed by RT-qPCR analysis of the tumor tissues (Fig. 4d). A cDNA microarray analysis was performed to compare gene expression profiles of tumors obtained from mice with or without Dox treatment. Partial lists of differentially expressed genes are shown in Fig. 4e (including the data of the control liver) and Table S2. Interestingly, Dox treatment reduced the mRNA expression of *Afp*, *Slpi*, *Gpc3*, and *H19*, which are expressed in the fetal/neonatal liver and activated in CCl_4- or diethylnitrosamine (DEN)-induced liver tumors.[26] The induction of MadMyc suppressed the mRNA expression of *S100a9* and *S100a8*, which encodes calprotectin,[27] a heterodimeric protumorigenic protein, as well as that of *Psat1* and *Phgdh* whose products are involved in serine biosynthesis. The detection of transcripts of the genes

for immunoglobulin and immune functions in the tumors was attributable to inflammatory cell infiltrates frequently found in the tumors with induced MadMyc (Fig. 4b). *Ppp1r3g*, *Slc1a2*, and *Cyp1a2* were identified as the genes that were suppressed in *AKT/HRAS*-induced tumors, but partially recovered by MadMyc induction. Gene Set Enrichment Analysis (GSEA) revealed that the expression dataset of the tumors was significantly enriched with the genes enumerated in the gene sets listed in the Myc Target Gene Database (Fig. 4f, Table S3a). Furthermore, the expression dataset was closely associated with the "lipid metabolism" (Fig. 4g, Table S3b) and "translation" (Fig. 4h, Table 3c) gene sets.

Overexpression of Myc enhances *AKT*- and/or *HRAS*-mediated hepatocarcinogenesis with suppression of lipid accumulation in tumor cells.

We then co-introduced *Myc* in combination with *AKT* (*AKT/Myc*), *HRAS* (*HRAS/Myc*), and *AKT* and *HRAS* (*AKT/HRAS/Myc*). Although injection of the *Myc*-expressing plasmid alone did not produce any tumors during the period of one year (data not shown), the co-introduction of *Myc* markedly enhanced tumorigenesis induced by *AKT* or *HRAS*, generating multiple liver tumors within 7-8 weeks (Fig. 5a). The combination of these three oncogenes (*AKT/HRAS/Myc*) induced numerous small liver tumors, which replaced whole livers as early as 2 weeks (Fig. 5a). Increased levels of *Myc* mRNA in these tumors were confirmed by RT-qPCR analysis (Supplementary Fig. 2). All these tumors showed the histology of HCC with prominent nucleoli (Fig. 5b, c). *AKT/HRAS/Myc*-induced tumors were the least differentiated and diffusely infiltrative. Although some cells in *AKT/Myc*-induced tumors showed marked lipid accumulation, *HRAS/Myc*- and *AKT/HRAS/Myc*-induced tumor cells were almost devoid of lipid (Fig. 5b). The tumor cells showed highly proliferative activities, with Ki-67-labeling indices of 71.3%, 80.7%, and 82.2% in *AKT/Myc*-, *HRAS/Myc*-, and *AKT/HRAS/Myc*-induced tumors, respectively (Fig. 5d). In contrast to the heterogeneous expression levels of Myc in *AKT/Myc*-induced tumors,

HRAS/Myc- and *AKT/HRAS/Myc*-induced tumor cells demonstrated strong and homogeneous Myc expression (Fig. 5b). In *AKT/Myc*-induced tumors, cells without lipid accumulation showed higher proliferative activity than those with abundant intracytoplasmic lipid (Fig. 5e). *HRAS/Myc*-induced tumors contained many apoptotic cells that were highlighted by cleaved caspase-3 immunohistochemistry (Fig 5b, c, f).

Adequate levels of Myc activation are required for the promotion of *AKT/HRAS*-induced hepatocarcinogenesis.

We further explored the dose-response relationship between the levels of Myc activation and its carcinogenic effect. In the *AKT/HRAS/Myc*-induced hepatocarcinogenesis model, the amount of introduced *Myc*-expressing plasmid was decreased to one-third (1/3×) or increased three times (3×) and compared the extent of tumor formation with the original (1×). Myc immunohistochemistry without TSA demonstrated that the introduction of more (3×) *Myc* increased Myc expression in the individual transduced hepatocytes at 3 days after the introduction of the plasmids (Supplementary Fig. 6a, b), although the total number of the HA-positive transduced cells was comparable to that seen in the mice in which 1× or 1/3× *Myc* was introduced (Supplementary Fig. 6a, c). Interestingly, the introduction of 3× *Myc* inhibited its tumor-promoting effect, whereas the effect was not affected by the decreased dosage (1/3×) of *Myc* (Fig. 6a), which was clearly exemplified by changes in relative liver weight (Fig. 6a, Supplementary Fig. 2c). Although HA-positive transduced cells formed coalescent tumors of poorly differentiated HCC when 1× or 1/3× *Myc* was introduced, the introduction of 3× *Myc* reduced the size and the number of tumors, resulting in discrete tumor nodules, which were composed of a thick trabecular structures surrounded by well developed sinusoids, suggesting a more differentiated state (Fig. 6b). Quantitative analysis of areas of HA-positive cells showed a biphasic dose response (Fig. 6c).

Myc immunohistochemistry without TSA revealed that Myc immunoreactivity was significantly higher in the tumors induced by the introduction of 3× *Myc* as compared with those induced by 1× or 1/3× *Myc* (Fig. 6b, Supplementary Fig. 7a). Myc overexpression did not affect the phosphorylation state of AKT (Fig. 6b, Supplementary Fig. 7b). Because Myc has also been shown to trigger apoptosis when activated, we suspected that Myc-induced apoptosis might be involved in dampening of the tumor-promoting effect when *Myc* was applied at high doses. Indeed, the average number of cleaved caspase-3-positive apoptotic cells 3 days following plasmid injection was twice as high in the liver infused with *Myc* (3×) as in the liver infused with *Myc* (1×) (Fig. 6d, e; Supplementary Fig. 6a).

Myc inhibits fatty acid synthesis and β-oxidation with potential interaction with HRAS.

We also explored the mRNA expression of genes relevant to fatty acid synthesis and degradation. In tumors induced by *AKT*, *HRAS*, and *AKT/HRAS*, the mRNA expression of proteins involved in fatty acid synthesis (Acly, Acaca, Fasn, Scd1, Scd2, and Srebf1) was increased compared with the control liver (Fig. 7). However, the increased expression was suppressed by the co-introduction of *Myc* particularly when *Myc* was combined with *HRAS* (Fig. 7). As for proteins related to transport of long-chain fatty acids (Cpt1a) and β-oxidation (Acadm, Hadha, Hadhb), the mRNA levels were markedly decreased in *HRAS/Myc*- and *AKT/HRAS/Myc*-induced tumors, but not in *AKT/Myc*-induced tumors (Fig. 7). These results suggested a potential synergistic interaction between Myc and HRAS in the suppression of fatty acid synthesis, transport, and β-oxidation. Compatible with the RT-qPCR data, proteomic analysis revealed that the expression of the critical enzymes in fatty acid synthesis, Acly and Fasn, was elevated in *AKT/HRAS*-induced tumors, but decreased in *AKT/HRAS/Myc*-induced tumors (Supplementary Fig. 8). The expression of many enzymes in fatty acid degradation was decreased in both tumors (Supplementary Fig. 8).

MYC-expressing human HCC is devoid of lipid accumulation and highly proliferative.

Finally, we inquired whether human HCC with MYC expression might demonstrate the phenotype similar to MYC-expressing mouse tumors. Among the 33 HCC cases examined, 9 cases demonstrated distinct nuclear MYC expression (Fig. 8a, b), although there was intratumoral heterogeneity. Tumors in 11 cases showing diffuse intracytoplasmic lipid accumulation of various degrees were completely negative for MYC (Fig. 8a, b). No MYC-positive tumor areas were accompanied with intracytoplasmic lipid accumulation (Fig. 8a) and a statistical analysis suggested that there was a nonrandom association between Myc expression and the lack of lipid accumulation (Fig. 8b; $P = 0.015$, Fisher's exact test). Interestingly, similar to Myc-overexpressing mouse tumors (see Fig. 5c), the nuclei of tumor cells with MYC expression contained prominent nucleoli (Fig. 8a). This tendency was confirmed by quantitative analysis (Fig. 9c; nucleolar size of control hepatocytes: 2.78 ± 0.17 μm^2). Furthermore, Ki-67 immunohistochemistry revealed that MYC-expressing HCC were more proliferative as compared with MYC-negative HCC with or without lipid accumulation (Fig. 8a, d).

DISCUSSION

Spontaneous posttranscriptional Myc activation occurred in *AKT/HRAS*-induced tumors. This was compatible with previous reports,[18] in which secondary Myc activation was described in liver tumors induced in *AKT/NRAS*-induced tumors. The Ras/MEK/ERK pathway has been shown to phosphorylate Ser-62 of MYC protein and enhance its stability.[6] The PI3K-mediated activation AKT has been demonstrated to inhibit glycogen synthase kinase-3, which phosphorylates MYC at Thr-58 and facilitates its proteasomal degradation.[6] The significance of these posttranslational regulation has been confirmed in mammary gland tumorigenesis *in vivo*.[28] It has also been demonstrated that RAS and AKT

induced both phosphorylation-dependent and -independent suppression of MAD, which inhibits MYC-mediated transcriptional activity.[29] In the present study, we found that increased Myc expression was closely associated with higher proliferative activity of tumor cells, suggesting an important role of Myc in the progression of mouse liver tumors. Intriguingly, malignant conversion of human hepatocarcinogenesis has been demonstrated to be associated with activation of the *MYC* transcription signature without concomitant overexpression of the *MYC* gene.[30]

AKT/HRAS-induced tumorigenesis was almost completely abrogated by the simultaneous introduction of *MadMyc* with these oncogenes, suggesting that low or basal levels of Myc expression facilitated the initiation step of *AKT/HRAS*-induced tumorigenesis. Interestingly, *KRAS*-driven mouse lung cancers, in which *Myc* is not amplified, have been reported to be contained and eradicated by the induction of a dominant-negative Myc mutant.[31] Furthermore, recent experiments using conditional *Myc*-knockout mice have shown the importance of expression of endogenous Myc in hepatocytic proliferation induced by a PPAR-α agonist and DEN-induced hepatocarcinogenesis.[32] We also showed that inhibition of secondary Myc activation by inducible MadMyc efficiently suppressed the progression of preneoplastic hepatocytes into fully proliferative neoplastic hepatocytes. Furthermore, MadMyc-mediated Myc suppression in *AKT/HRAS*-induced neoplastic hepatocytes decreased their proliferative activity. It has been shown that conditional Myc inactivation induces differentiation and tumor dormancy in mouse HCC induced by overexpression of Myc.[33] These results suggest that, although therapeutic interventions through Myc suppression are effective in the earlier phases of hepatocarcinogenesis, they might be also applicable to the established tumors.

MadMyc-mediated inhibition of proliferation of *AKT/HRAS*-induced tumors was associated with the reduced expression of several genes (*Afp*, *Slpi*, *Gpc3*, and *H19*) with oncofetal features.[26] Although the exact functions of these genes in hepatocarcinogenesis remain elusive, our results suggest that the regulation of the expression of fetal/neonatal liver genes by Myc may be important in HCC cell proliferation. *S100a8* and *S100a9*, encoding calprotectin, were also identified to be suppressed by MadMyc induction. Calprotectin has recently been shown to play a protumorigenic function in DEN-induced mouse hepatocarcinogenesis.[27] Our results also demonstrated that the mRNA expression of *Psat1* and *Phgdh* was suppressed by MadMyc induction, suggesting that serine biosynthesis, which is crucial in glutathione synthesis,[34] could be a therapeutic target. On the other hand, MadMyc induction recovered the mRNA expression of *Cyp1a2* and *Ppp1r3g*. Interestingly, cytochrome P450 1A2, the product of *CYP1A2*, which metabolizes 17-β-estradiol to 2-methoxyestradiol, has been demonstrated to be decreased in human HCC.[35] *Ppp1r3g*, encoding a glycogen-targeting subunit of protein phosphatase 1 that dephosphorylates and activates glycogen synthase, is involved in glucose homeostasis and lipid metabolism.[36] Furthermore, GSEA revealed that MadMyc induction was closely correlated with enhanced lipid synthesis and reversely correlated with protein translation, highlighting the importance of therapeutic reversal of metabolic reprogramming induced by Myc.

When *Myc* was overexpressed simultaneously with *AKT*, *HRAS*, or *AKT/HRAS*, it dramatically facilitated tumorigenesis. The synergistic interaction between transgenic *Myc* and *Hras* has been shown in mouse hepatocarcinogenesis.[11] Furthermore, in a transgenic mouse model overexpressing both Myc and transforming growth factor-α, liver tumorigenesis has been reported to be facilitated due to the generation of an oxidative stress environment that causes the accumulation of DNA damage.[37] However, rapid induction of liver tumors in our experiments suggests more direct interactions of Myc and these

oncogenic pathways, such as cross signaling between epidermal growth factor receptor and Myc, which has been found in mutant KRAS-induced pancreatic tumors.[38] Although deregulated Myc is also a well-known inducer of apoptosis in cells with intact ARF/p53 function,[39] the activation of AKT signaling has been shown to inhibit apoptosis induced by Myc,[40] sparing its growth-promoting effects.

Our results also revealed that concomitant *Myc* overexpression above specific threshold levels suppressed *AKT/HRAS*-induced hepatocarcinogenesis with an increase in early apoptotic cell death of transduced hepatocytes. Consistent with our findings, Murphy et al.[41] Reported that low levels of deregulated Myc induced ectopic proliferation of somatic cells including hepatocytes and that higher levels of Myc expression triggered ARF/p53 apoptotic pathways. Similar differential dose effects of MYC were found in human hepatocellular carcinoma cell lines with various levels of induced Myc expression.[42] Our data show for the first time that the extent of hepatocarcinogenesis is significantly influenced by the levels of deregulated Myc expression, with lower levels being more efficient.

Intracytoplasmic lipid was lost in highly proliferative cells with Myc expression in *AKT/HRAS*-induced tumors and in tumor cells with forced *Myc* expression. Although the mRNA expression of proteins involved in fatty acid synthesis was increased in *AKT*- and/or *HRAS*-induced tumors, it was strongly suppressed by forced Myc expression. The mRNA expression, as well as protein expression, of the major enzymes participating in β-oxidation was suppressed in tumors, especially in those induced by the combination of *HRAS* and *Myc*. Although Myc has been known to stimulate lipogenesis and β-oxidation,[2] our results clearly demonstrated a novel interaction of these oncogenes in metabolic reprogramming in hepatocytic tumors. Interestingly, in *MYCN*-amplified neuroblastoma cell lines, inhibition of N-Myc results in the accumulation of lipid droplets.[43] Because the proliferative activity

observed in *AKT/HRAS/Myc*-induced tumors, in which both fatty acid synthesis and β-oxidation were profoundly suppressed, was the highest, this metabolic reprogramming might be beneficial for tumor cell proliferation.

MYC-positive human HCC cells lacked intracytoplasmic lipid accumulation and were more proliferative as compared with those without MYC expression. A previous report demonstrated that MYC gene amplification in human HCC was positively correlated with proliferative activity and associated with shorter disease-free survival in patients.[44] Furthermore, MYC-positive tumor cells characteristically possessed prominent nucleoli, which were similar to those found in the nuclei of Myc-overexpressing mouse tumors. MYC is known to be involved in synthesis of the precursor rRNA and its processing.[45] Interestingly, adenovirus-mediated overexpression of Myc in mouse hepatocytes *in vivo* has been reported to induce enlargement of their nucleoli, as well as nuclei, with increased mRNA levels of genes that encode proteins engaged in ribosomal biogenesis and protein translation.[46] In conclusion, our findings in this experimental study, which have been at least partly validated in human specimens, highlight the critical importance of Myc in hepatocarcinogenesis.

MATERIALS AND METHODS

Animals

C57BL/6J mice were purchased from Charles River Laboratories Japan (Yokohama, Japan). The mice were euthanized under deep anesthesia. The protocols used for animal experimentation were approved by the Animal Research Committee, Asahikawa Medical University, and all animal experiments adhered to the criteria outlined in the Animal Research: Reporting of In Vivo Experiments (ARRIVE)

guidelines. No blinding was used for animal experiments. All animals used were included in the analyses.

Transposon-mediated introduction of oncogenes into mouse hepatocytes

To introduce genes into hepatocytes *in vivo*, the combination of the SB transposon system and HTVi was performed.[47] The plasmids were co-injected with a SB13 transposase-expression plasmid into male C57BL/6J mice (8-12-week-old) via HTVi. An SB13 transposase-expressing vector (pT2/C-Luc/PGK-SB13, Addgene plasmid #20207) and a myrAKT-HA-expressing transposon cassette vector (pT3-EF1α-myrAKT-HA, Addgene plasmid #31789) were obtained from Addgene (Cambridge, MA). cDNA fragments of FLAG-HRAS^{V12}, EGFP, Venus-IRES-rtTA3, and MadMyc-HA were amplified from pTomo-Ras (Addgene plasmid #26292), pCMV-EGFP (Takara Bio, Kusatsu, Shiga, Japan), TtRMPVIR (Addgene plasmid #27995), and MadMyc-HA (Addgene plasmid #16557),[25] respectively. A full length Myc fragment was amplified from cDNA of diethylnitrosamine-induced mouse liver tumors. These cDNA fragments were cloned into the pT3-EF1α transposon cassette plasmid using the Gateway® cloning system (ThermoFisher Scientific, Waltham, MA). For construction of the tetracycline-controlled transcriptional activation system (Tet-On), the EF1α promoter of the destination vector of the Gateway cloning system was replaced with the TRE-tight promoter, which was amplified from TtRMPVIR, using the GeneArt Seamless Cloning and Assembly Kit (Thermo Fisher Scientific, Waltham, MA).

For HTVi, plasmids were dissolved in 2.5 mL Ringer solution and rapidly injected via the lateral tail vein of mice within 8 seconds. The total amount of plasmid DNA were 16, 25, 36, and 43 μg for mixtures of 2, 3, 4, and 5 different plasmids (including the transposase-expressing vector), respectively. The molar ratio of the transposase-expressing vector to each transposon cassette plasmid containing

various genes was 1:2. To induce MadMyc expression in the Tet-On system, mice were given Dox *ad libitum* as drinking water (2 mg/mL Dox and 1% sucrose in tap water). The animals were randomly assigned to Dox (-) and Dox (+) groups.

Microscopic examination and immunohistochemistry

The livers were fixed in phosphate-buffered 4% paraformaldehyde for 24 hours, dehydrated, cleared, and embedded in paraffin. Immunohistochemical staining was performed using the EnVision/HRP system (DAKO, Carpinteria, CA) on deparaffinized sections treated with Target Retrieval Solution (DAKO). The antibodies used were as follows: anti-GFP (A-11122, ThermoFisher Scientific), anti-p-AKT (#3787, Cell Signaling Technology, Danvers, MA), anti-p-ERK1/2 (#4370, Cell Signaling Technology), anti-Myc (Abcam 32072, Cambridge, UK), anti-Ki-67 (Nichirei, Tokyo, Japan), anti-cleaved caspase-3 (#9661, Cell signaling Technology), anti-hemagglutinin (HA) (Roche Diagnostics), anti-p16 (M-156) (sc-1207, Santa Cruz Biotechnology, Santa Cruz, CA), and p21 (F-5) (sc-6246, Santa Cruz). The chromogen 3,3'-diaminobenzidine tetrahydrochloride (Vector Laboratories, Burlingame, CA) and HistoGreen (LINARIS Biologische Produkte, Dossenheim, Germany) were used for signal detection. For the detection of Myc in some experiments, tyramide signal amplification (TSA) was performed using the TSA Plus DIG Kit (PerkinElmer, Waltham, MA). Morphometric analyses were performed using ImageJ software. Frozen sections were stained with Sudan III.

Quantitative reverse transcriptase-polymerase chain reaction (RT-qPCR)

Total RNA was extracted from frozen liver tissues and subjected to RT-qPCR analyses, which were performed using the ΔΔCt method with the FastStart Universal SYBR Green Master Mix (Roche Diagnostics, Mannheim, Germany). Each reaction was performed in duplicate, and the mRNA levels

were normalized against β-actin (*Actb*). The sequences of the specific primers are listed in Supplementary Table 1.

Microarray and gene set enrichment analysis (GSEA)

Total RNA was prepared from snap-frozen tissues using a Sepasol reagent (RNA I Super G; Nacalai Tesque, Kyoto, Japan) and samples with an RNA integrity number >7.0 were used for microarray analyses. Samples of AKT/HRAS/Tet-On-MadMyc tumors (a mixture of 3 independent tumors) either from mice treated or not treated with Dox were analyzed and compared by one-color microarrays (3D-Gene Microarray, TORAY, Tokyo, Japan). After background subtraction, the raw microarray data were normalized using a standard global normalization technique. GSEA was performed using the GSEA v2.2.3 software using gene set collections of "MYC Target Gene Database" (C2), "Reactome gene sets" (C2), and "GO gene sets" (C5) from the Molecular Signature Database provided by the Broad Institute.[48]

Proteomic analysis of the enzymes involved in fatty acid metabolism

Samples for soluble proteins were extracted from the tumors induced by *AKT/HRAS* (a mixture of 4 tumors) and *AKT/HRAS/Myc* (a mixture of 5 tumors), as well as control liver tissues (a mixture of tissue fragments from 4 mice). The samples were digested by trypsin and subjected to triplicate liquid chromatography-tandem mass spectrometry analyses (LTQ-Orbitrap XL, Thermo Fisher Scientific, San Jose, CA). Proteins were identified by the Mascot software (Matrix Science, London, UK) and the spectral counting data were semiquantitatively represented as exponentially modified protein abundance index (emPAI).

Human liver samples

The retrospective analysis of surgical specimens was approved by the internal review board of Asahikawa Medical University (approved number: 14004). A total of 33 HCC samples from patients who had curative hepatectomy were collected. Myc and Ki-67 immunohistochemistry was performed as described above using serial paraffin sections.

Statistical analysis

Results from experiments were expressed as mean ± SEM. Unpaired two-tailed *t*-test, Mann-Whitney *U*-test, Kruskal-Wallis test, one-way analysis of variance (ANOVA) with Tukey post-hoc test , or Mantel-Cox test (for a Kaplan-Meier plot) were performed to compare differences. Fisher's exact test was used to evaluate human HCC samples. Statistical analyses were performed using Prism 6.07 (GraphPad Software, La Jolla, CA).

CONFLICTS OF INTEREST

The authors declare no conflict of interest.

ACKNOWLEDGEMENTS

This work was supported by grants from the Ministry of Education, Culture, Sports, Science, and Technology of Japan (#26870025 to MY; #18590362, #21590426, and #24390092 to YN). We thank Mr. Yoshiyasu Satake for animal care and Ms. Ema Yamatomi, Ms. Hiroko Chiba, and Ms. Aya Kitano for secretarial assistance. We are also grateful to the staff of the Department of Pathology, Asahikawa Medical University Hospital for generous help.

REFERENCES

1 Stine ZE, Walton ZE, Altman BJ, Hsieh AL, Dang CV. MYC, Metabolism, and Cancer. Cancer Discov 2015; 5: 1024-1039.

2 Wahlstrom T, Henriksson MA. Impact of MYC in regulation of tumor cell metabolism. Biochim Biophys Acta 2015; 1849: 563-569.

3 Zucman-Rossi J, Villanueva A, Nault JC, Llovet JM. Genetic landscape and biomarkers of hepatocellular carcinoma. Gastroenterology 2015; 149: 1226-1239 e1224.

4 Fujiwara Y, Monden M, Mori T, Nakamura Y, Emi M. Frequent multiplication of the long arm of chromosome 8 in hepatocellular carcinoma. Cancer Res 1993; 53: 857-860.

5 Thorgeirsson SS, Grisham JW. Molecular pathogenesis of human hepatocellular carcinoma. Nat Genet 2002; 31: 339-346.

6 Sears RC. The life cycle of c-myc: from synthesis to degradation. Cell Cycle 2004; 3: 1133-1137.

7 Adhikary S, Eilers M. Transcriptional regulation and transformation by Myc proteins. Nat Rev Mol Cell Biol 2005; 6: 635-645.

8 Lutz W, Leon J, Eilers M. Contributions of Myc to tumorigenesis. Biochim Biophys Acta 2002; 1602: 61-71.

9 Carroll M, Borden KL. The oncogene eIF4E: using biochemical insights to target cancer. J Interferon Cytokine Res 2013; 33: 227-238.

10 Poortinga G, Quinn LM, Hannan RD. Targeting RNA polymerase I to treat MYC-driven cancer. Oncogene 2015; 34: 403-412.

11 Sandgren EP, Quaife CJ, Pinkert CA, Palmiter RD, Brinster RL. Oncogene-induced liver neoplasia in transgenic mice. Oncogene 1989; 4: 715-724.

12 Coulouarn C, Gomez-Quiroz LE, Lee JS, Kaposi-Novak P, Conner EA, Goldina TA *et al*. Oncogene-specific gene expression signatures at preneoplastic stage in mice define distinct mechanisms of hepatocarcinogenesis. Hepatology 2006; 44: 1003-1011.

13 Stein TJ, Bowden M, Sandgren EP. Minimal cooperation between mutant Hras and c-myc or TGFalpha in the regulation of mouse hepatocyte growth or transformation in vivo. Liver Int 2011; 31: 1298-1305.

14 Ivics Z, Hackett PB, Plasterk RH, Izsvak Z. Molecular reconstruction of Sleeping Beauty, a Tc1-like transposon from fish, and its transposition in human cells. Cell 1997; 91: 501-510.

15 Liu F, Song Y, Liu D. Hydrodynamics-based transfection in animals by systemic administration of plasmid DNA. Gene Ther 1999; 6: 1258-1266.

16 Yant SR, Meuse L, Chiu W, Ivics Z, Izsvak Z, Kay MA. Somatic integration and long-term transgene expression in normal and haemophilic mice using a DNA transposon system. Nat Genet 2000; 25: 35-41.

17 Carlson CM, Frandsen JL, Kirchhof N, McIvor RS, Largaespada DA. Somatic integration of an oncogene-harboring Sleeping Beauty transposon models liver tumor development in the mouse. Proc Natl Acad Sci U S A 2005; 102: 17059-17064.

18 Ho C, Wang C, Mattu S, Destefanis G, Ladu S, Delogu S *et al*. AKT (v-akt murine thymoma viral oncogene homolog 1) and N-Ras (neuroblastoma ras viral oncogene homolog) coactivation in the mouse liver promotes rapid carcinogenesis by way of mTOR (mammalian target of rapamycin complex 1), FOXM1 (forkhead box M1)/SKP2, and c-Myc pathways. Hepatology 2012; 55: 833-845.

19 Calvisi DF, Wang C, Ho C, Ladu S, Lee SA, Mattu S *et al*. Increased lipogenesis, induced by AKT-mTORC1-RPS6 signaling, promotes development of human hepatocellular carcinoma. Gastroenterology 2011; 140: 1071-1083.

20 Chow EK, Fan LL, Chen X, Bishop JM. Oncogene-specific formation of chemoresistant murine hepatic cancer stem cells. Hepatology 2012; 56: 1331-1341.

21 Kang TW, Yevsa T, Woller N, Hoenicke L, Wuestefeld T, Dauch D *et al*. Senescence surveillance of pre-malignant hepatocytes limits liver cancer development. Nature 2011; 479: 547-551.

22 Castellano E, De Las Rivas J, Guerrero C, Santos E. Transcriptional networks of knockout cell lines identify functional specificities of H-Ras and N-Ras: significant involvement of N-Ras in biotic and defense responses. Oncogene 2007; 26: 917-933.

23 Castellano E, Guerrero C, Nunez A, De Las Rivas J, Santos E. Serum-dependent transcriptional networks identify distinct functional roles for H-Ras and N-Ras during initial stages of the cell cycle. Genome Biol 2009; 10: R123.

24 Berns K, Hijmans EM, Bernards R. Repression of c-Myc responsive genes in cycling cells causes G1 arrest through reduction of cyclin E/CDK2 kinase activity. Oncogene 1997; 15: 1347-1356.

25 Hermeking H, Rago C, Schuhmacher M, Li Q, Barrett JF, Obaya AJ *et al*. Identification of CDK4 as a target of c-MYC. Proc Natl Acad Sci U S A 2000; 97: 2229-2234.

26 Chen X, Yamamoto M, Fujii K, Nagahama Y, Ooshio T, Xin B *et al*. Differential reactivation of fetal/neonatal genes in mouse liver tumors induced in cirrhotic and non-cirrhotic conditions. Cancer Sci 2015; 106: 972-981.

27 De Ponti A, Wiechert L, Schneller D, Pusterla T, Longerich T, Hogg N *et al*. A pro-tumorigenic function of S100A8/A9 in carcinogen-induced hepatocellular carcinoma. Cancer Lett 2015; 369: 396-404.

28 Wang X, Cunningham M, Zhang X, Tokarz S, Laraway B, Troxell M *et al*. Phosphorylation regulates c-Myc's oncogenic activity in the mammary gland. Cancer Res 2011; 71: 925-936.

29 Zhu J, Blenis J, Yuan J. Activation of PI3K/Akt and MAPK pathways regulates Myc-mediated transcription by phosphorylating and promoting the degradation of Mad1. Proc Natl Acad Sci U S A 2008; 105: 6584-6589.

30 Kaposi-Novak P, Libbrecht L, Woo HG, Lee YH, Sears NC, Coulouarn C *et al*. Central role of c-Myc during malignant conversion in human hepatocarcinogenesis. Cancer Res 2009; 69: 2775-2782.

31 Soucek L, Whitfield JR, Sodir NM, Masso-Valles D, Serrano E, Karnezis AN *et al*. Inhibition of Myc family proteins eradicates KRas-driven lung cancer in mice. Genes Dev 2013; 27: 504-513.

32 Qu A, Jiang C, Cai Y, Kim JH, Tanaka N, Ward JM *et al*. Role of Myc in hepatocellular proliferation and hepatocarcinogenesis. J Hepatol 2014; 60: 331-338.

33 Shachaf CM, Kopelman AM, Arvanitis C, Karlsson A, Beer S, Mandl S *et al*. MYC inactivation uncovers pluripotent differentiation and tumour dormancy in hepatocellular cancer. Nature 2004; 431: 1112-1117.

34 Antonov A, Agostini M, Morello M, Minieri M, Melino G, Amelio I. Bioinformatics analysis of the serine and glycine pathway in cancer cells. Oncotarget 2014; 5: 11004-11013.

35 Ren J, Chen GG, Liu Y, Su X, Hu B, Leung BC *et al*. Cytochrome P450 1A2 Metabolizes 17beta-Estradiol to Suppress Hepatocellular Carcinoma. PLoS One 2016; 11: e0153863.

36 Zhang Y, Xu D, Huang H, Chen S, Wang L, Zhu L *et al*. Regulation of glucose homeostasis and lipid metabolism by PPP1R3G-mediated hepatic glycogenesis. Mol Endocrinol 2014; 28: 116-126.

37 Factor VM, Kiss A, Woitach JT, Wirth PJ, Thorgeirsson SS. Disruption of redox homeostasis in the transforming growth factor-alpha/c-myc transgenic mouse model of accelerated hepatocarcinogenesis. J Biol Chem 1998; 273: 15846-15853.

38 Diersch S, Wirth M, Schneeweis C, Jors S, Geisler F, Siveke JT *et al*. Kras induces EGFR-MYC cross signaling in murine primary pancreatic ductal epithelial cells. Oncogene 2015; doi: 10.1038/onc.2015.437.

39 Hoffman B, Amanullah A, Shafarenko M, Liebermann DA. The proto-oncogene c-myc in hematopoietic development and leukemogenesis. Oncogene 2002; 21: 3414-3421.

40 Kauffmann-Zeh A, Rodriguez-Viciana P, Ulrich E, Gilbert C, Coffer P, Downward J *et al*. Suppression of c-Myc-induced apoptosis by Ras signalling through PI(3)K and PKB. Nature 1997; 385: 544-548.

41 Murphy DJ, Junttila MR, Pouyet L, Karnezis A, Shchors K, Bui DA *et al*. Distinct thresholds govern Myc's biological output in vivo. Cancer Cell 2008; 14: 447-457.

42 Akita H, Marquardt JU, Durkin ME, Kitade M, Seo D, Conner EA *et al*. MYC activates stem-like cell potential in hepatocarcinoma by a p53-dependent mechanism. Cancer Res 2014; 74: 5903-5913.

43 Zirath H, Frenzel A, Oliynyk G, Segerstrom L, Westermark UK, Larsson K *et al*. MYC inhibition induces metabolic changes leading to accumulation of lipid droplets in tumor cells. Proc Natl Acad Sci U S A 2013; 110: 10258-10263.

44 Kawate S, Fukusato T, Ohwada S, Watanuki A, Morishita Y. Amplification of c-myc in hepatocellular carcinoma: correlation with clinicopathologic features, proliferative activity and p53 overexpression. Oncology 1999; 57: 157-163.

45 Schlosser I, Holzel M, Murnseer M, Burtscher H, Weidle UH, Eick D. A role for c-Myc in the regulation of ribosomal RNA processing. Nucleic Acids Res 2003; 31: 6148-6156.

46 Kim S, Li Q, Dang CV, Lee LA. Induction of ribosomal genes and hepatocyte hypertrophy by adenovirus-mediated expression of c-Myc in vivo. Proc Natl Acad Sci U S A 2000; 97: 11198-11202.

47 Bell JB, Podetz-Pedersen KM, Aronovich EL, Belur LR, McIvor RS, Hackett PB. Preferential delivery of the Sleeping Beauty transposon system to livers of mice by hydrodynamic injection. Nat Protoc 2007; 2: 3153-3165.

48 Subramanian A, Tamayo P, Mootha VK, Mukherjee S, Ebert BL, Gillette MA *et al*. Gene set enrichment analysis: a knowledge-based approach for interpreting genome-wide expression profiles. Proc Natl Acad Sci U S A 2005; 102: 15545-15550.

FIGURE LEGENDS

Fig. 1 Introduction of *AKT* or *HRAS* into mouse hepatocytes induces liver tumors after long periods of incubation.

The pathological features of the liver tumors induced by activated *myrAKT* (*AKT*) or $HRAS^{V12}$ (*HRAS*) (incubation periods: *AKT*-induced tumors, 28 weeks; *HRAS*-induced tumors, 20 weeks). (a) Gross appearances of the livers. (b) Hematoxylin and eosin (H&E) and Sudan III stainings of the liver. The tumors show features of hepatocellular carcinoma (HCC) associated with lipid accumulation. T, tumors. Scale bar, 50 μm. (c) Immunohistochemistry for phosphorylated AKT (pAKT), phosphorylated ERK1/2 (pERK1/2), and Myc (with TSA). T, tumors. Scale bar, 50 μm.

Fig. 2 Cointroduction of *AKT* and *HRAS* into mouse hepatocytes rapidly induces liver tumors with spontaneous Myc expression.

(a) Gross appearances of the livers. Note the white discoloration and multiple large tumors 4 and 8 weeks after introduction of both *AKT* and *HRAS*. (b) H&E staining of the liver. Preneoplastic hepatocytes containing abundant intracytoplasmic lipid found after 2 weeks develop into microscopic (4 weeks) and macroscopic (8 weeks) tumors with typical histology of HCC. The tumors consist of cells with (white arrowheads) and without (black arrowheads) lipid accumulation. (c) Immunohistochemistry for Ki-67 comparing *AKT*-, *HRAS*-, and *AKT/HRAS*-induced tumors. The cells in *AKT/HRAS*-induced tumors, particularly those without lipid accumulation, show higher levels of Ki-67 labeling. (d) Quantitative analysis of Ki-67-labeled tumor cells in *AKT*-, *HRAS*-, and *AKT/HRAS*-induced tumors (n = 10, 12, and 14, respectively). (e) Quantitative analysis of Ki-67-labeling in tumor cells with or without intracytoplasmic lipid accumulation in *AKT/HRAS*-induced tumors. (f) Myc immunohistochemistry with TSA of *AKT/HRAS*-induced tumors. Some of tumor cells without intracytoplasmic lipid accumulation

show nuclear Myc expression. (g) Quantitative analysis of Myc protein expression in tumor cells with or without intracytoplasmic lipid accumulation in *AKT/HRAS*-induced tumors. (h) Myc/Ki-67 double immunohistochemistry of *AKT/HRAS*-induced tumors. Note the many tumor cells positive for both Myc (brown) and Ki-67 (green) (black arrowheads). (i) Quantitative analysis of Ki-67-labeling in tumor cells with or without Myc expression in *AKT/HRAS*-induced tumors. T: tumors. Scale bar, 50 μm. Statistical analyses: Kruskal-Wallis test (d), Mann-Whitney *U*-test (e, g, i). NS, not significant. **P*<0.05, ***: *P*<0.001, ****: *P*<0.0001.

Fig. 3 Competitive inhibition of Myc impairs *AKT/HRAS*-induced tumorigenesis.

(a) Gross appearances of the livers 6 weeks after introduction of *AKT/HRAS* with or without *MadMyc*. (b) H&E staining and immunohistochemistry for HA of the liver. (c) Quantitative analyses of the area containing HA-positive transduced cells (n = 3 for *AKT/HRAS* group, n = 6 for *AKT/HRAS/MadMyc* group). A total area of approximately 12 mm^2 was analyzed in each animal. (d) Gross appearances of the livers and liver-to-body weight ratios 4 weeks after the introduction of *AKT/HRAS*/Tet-On-*MadMyc*. In the Dox (+) group, at 2 weeks after plasmid injection, Dox was administered during a period of 2 weeks to induce MadMyc (n = 6 for each group). (e) H&E and Sudan III stainings, double immunohistochemistry for Ki-67 (brown) and HA (green), and immunohistochemistry for phosphorylated AKT (pAKT) of the livers. (f) Quantitative analysis of percentages of area containing HA-positive transduced cells. A total area of 2.32 mm^2 was analyzed in each animal. (g, h) HA-positive cells with lipid droplets (g), and double positive cells for Ki-67 and HA (h) in the Dox (-) and Dox (+) groups (n = 6 and 4, respectively). Approximately 500 HA-positive cells were analyzed in each animal (g, h). T, tumors. Scale bar, 50 μm. Statistical analyses: unpaired *t*-test (d and f), Mann-Whitney *U*- test (c, g, and h). **P*<0.05, **: *P*<0.01.

Fig. 4 Competitive inhibition of Myc inhibits the proliferative activity of *AKT/HRAS*-induced tumors.

(a) Gross appearances of the livers and liver-to-body weight ratios 6 weeks after the introduction of *AKT/HRAS/*Tet-On-*MadMyc*. In the Dox (+) group, at 4 weeks after plasmid injection, Dox was administered during a period of 2 weeks to induce MadMyc (n = 5 for Dox [-] group, n = 3 for Dox [+] group). (b) H&E staining and immunohistochemistry for Ki-67 of the liver. Intracytoplasmic lipid accumulation is more prominent in tumor cells in the Dox (+) group. There are scattered foci of lymphoplasmacytic infiltration in the stroma (arrows). (c) Quantitative analysis of Ki-67-labeling in tumor cells (10 tumor nodules were examined in each group). (d) RT-qPCR analysis of MadMyc mRNA expression in tumors (n = 5 for Dox [-] group, n = 8 for Dox [+] group). (e) cDNA microarray analysis of control liver and tumors in the Dox (-) and Dox (+) groups. (e-h) GSEA results showing significant correlations of the expression dataset of the tumors with a "Myc target" gene set (f), a "lipid metabolism" gene set (g), and a "translation" gene set (h). For the Reactome gene sets and GO gene sets, those with subset size less than 100 were excluded. From 10837 probe sets with gene expression value greater than 25, 7348 known genes were selected by the symbol identifier and used as the expression dataset. Scale bar, 50 μm. Statistical analyses: unpaired *t*-test (a, c, and d). NS, not significant. ***: $P<0.001$, ****: $P<0.0001$.

Fig. 5 Overexpression of *Myc* enhances *AKT*- and/or *HRAS*-mediated hepatocarcinogenesis with suppression of lipid accumulation in tumor cells.

(a) Gross appearances of the livers after introduction of *AKT/Myc*, *HRAS/Myc*, and *AKT/HRAS/Myc*. Although multiple liver tumors were generated after 7-8 weeks when *AKT/Myc* or *HRAS/Myc* was

introduced, the combination of three oncogenes (*AKT/HRAS/Myc*) induced diffuse liver tumors as early as 2 weeks. (b) H&E staining and immunohistochemistry for Ki-67, Myc (with TSA), and cleaved caspase-3 of the livers 8, 7, and 2 weeks after the introduction of *AKT/Myc*, *HRAS/Myc* and *AKT/HRAS/Myc*, respectively. T: tumors. Scale bar, 50 μm. (c) H&E staining of the normal liver and tumors with *Myc* overexpression (higher magnification). White arrowheads indicate apoptotic cells in *HRAS/Myc*-induced tumors. Scale bar, 20 μm. (d) Comparison of cell proliferative activities (percentages of Ki-67-positive cells) among *AKT/Myc*-, *HRAS/Myc*-, and *AKT/HRAS/Myc*-induced liver tumors (n = 9, 11, and 15, respectively). (e) Relationship between the proliferative activity and lipid accumulation in *AKT/Myc*-induced tumors. (f) Quantitative analysis of the number of cleaved caspase 3-positive tumor cells per high power field (HPF). Statistical analyses: Kruskal-Wallis test (d, f), unpaired *t*-test (e). **P*<0.05, ***P*<0.01, *****P*<0.0001.

Fig. 6 The tumor-promoting effect of Myc overexpression is dependent on its degree of deregulation.

(a) Gross appearances of the livers and liver-to-body weight ratios 2 weeks after introduction of *AKT/HRAS* along with various doses of Myc (0, 1/3×, 1×, and 3× of the original dose used in the previous experiments). (b) H&E staining and immunohistochemistry for HA, Myc (without TSA), and phosphorylated AKT of the livers (2 weeks after the introduction of the indicated oncogenes). (c) Quantitative analyses of the area containing HA-positive transduced cells (2 weeks after the introduction of the indicated oncogenes) (n = 6 in each group). A total area of approximately 32 mm^2 was analyzed in each animal. (d) Double immunohistochemistry for cleaved caspase-3 and HA of the livers 3 days after the introduction of *AKT/HRAS/Myc* (1×) or *AKT/HRAS/Myc* (3×). (e) Quantification of cleaved caspase-3 and HA double-positive cells in *AKT/HRAS/Myc* (1×)- and *AKT/HRAS/Myc* (3×)-induced tumors.

Approximately 500 HA-positive cells were analyzed in each animal. Scale bar, 50 μm. Statistical analyses: one-way ANOVA with Tukey post-hoc test (a, c), Mann-Whitney *U*-test (e). **P*<0.05, ****P*<0.001, *****P*<0.0001.

Fig. 7 The combination of *Myc* and *HRAS* inhibits mRNA expression of proteins involved in fatty acid synthesis and degradation.

RT-qPCR analyses of mRNA expression of proteins involved in fatty acid synthesis (Acly, Acaca, Fasn, Scd1, Scd2, Srebf1), transport of long-chain fatty acids (Cpt1a), and fatty acid degradation (Acadm, Hadha, Hadhb) in control liver (Liver) and liver tumors induced by the introduction of various oncogenes (*AKT*, *AKT/Myc*, *HRAS*, *HRAS/Myc*, *AKT/HRAS*, *AKT*/*HRAS/Myc*) (n = 7-8 in each group). Statistical analyses: Mann-Whitney *U*-test. **P*<0.05, ***P*<0.01, ****P*<0.001, *****P*<0.0001.

Fig. 8 MYC-expressing human HCC lacks intracytoplasmic lipid accumulation and is highly proliferative.

(a) H&E staining and immunohistochemistry for MYC and Ki-67 of human HCC. Most tumor cells in the case #1 contain intracytoplasmic lipid droplets, while tumors in the cases #2-4 lack intracytoplasmic lipid accumulation. MYC is negative in the cases #1 and 2, while positive in the cases #3 and 4. Scale bar, 50 μm. (b) The relationship between lipid accumulation and nuclear MYC expression in HCC. (c, d) Comparison of nucleolar sizes (c) and cell proliferative activities (percentages of Ki-67-positive cells) (d) among lipid-positive/MYC-negative HCC (n = 13), lipid–negative/MYC-negative HCC (n = 11), and lipid-negative/MYC-positive HCC (n = 9). Statistical analyses: Fisher's exact test (b) and Kruskal-Wallis test (c, d). **P*<0.05, ***P*<0.01, ****P*<0.001.

Fig. 1 (Xin et al.)

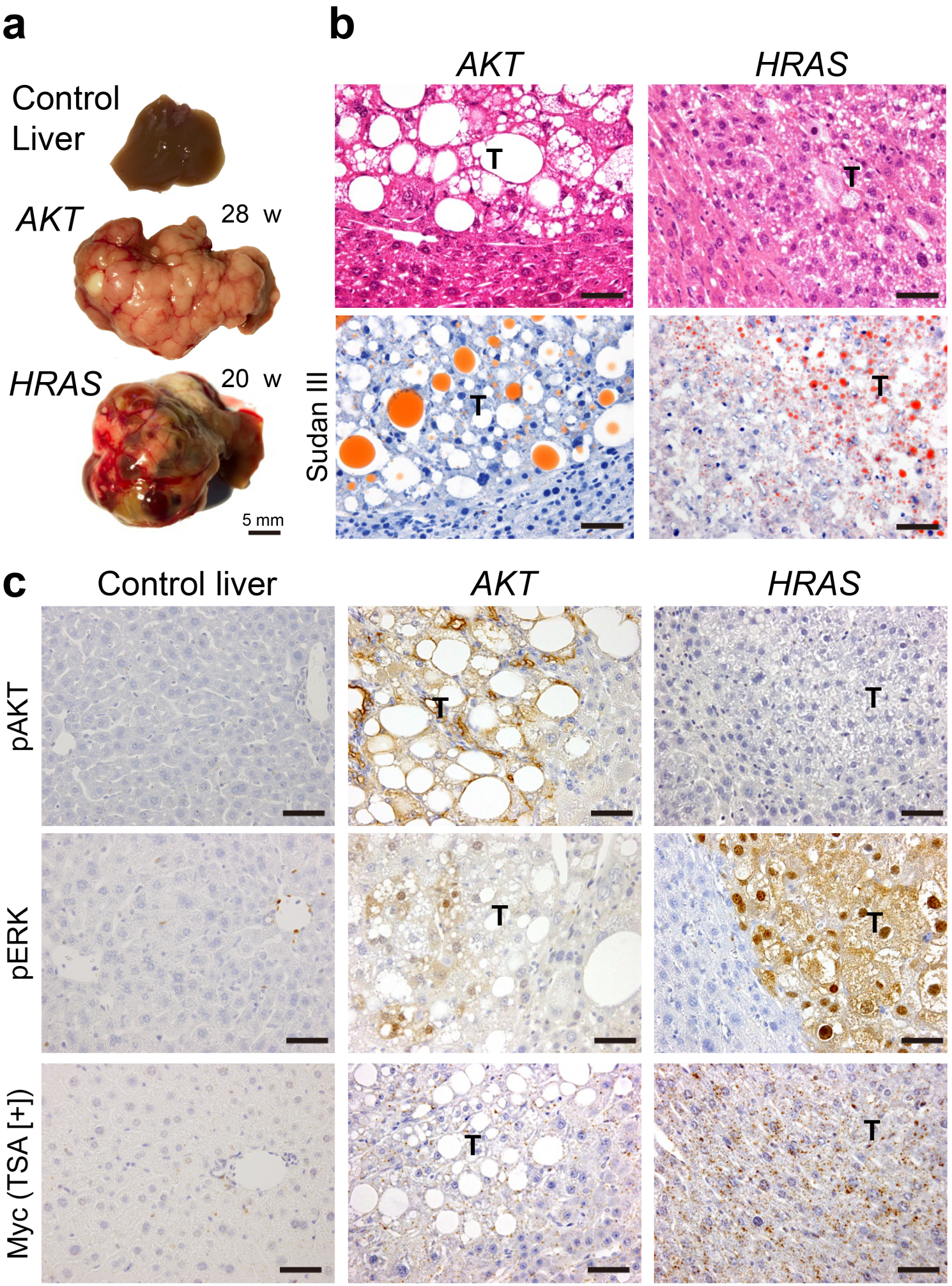

Fig. 2 (Xin et al.)

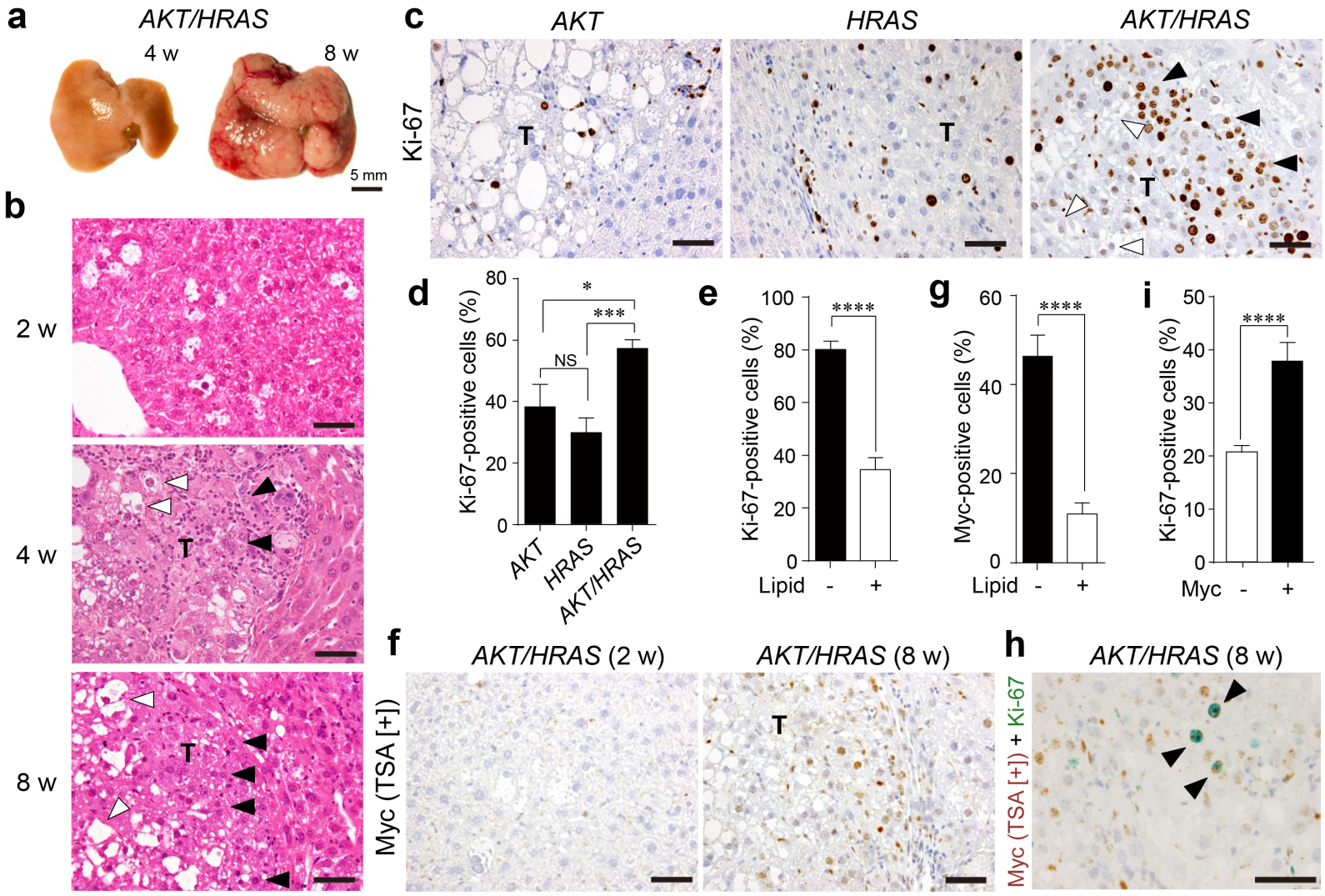

Fig. 3 (Xin et al.)

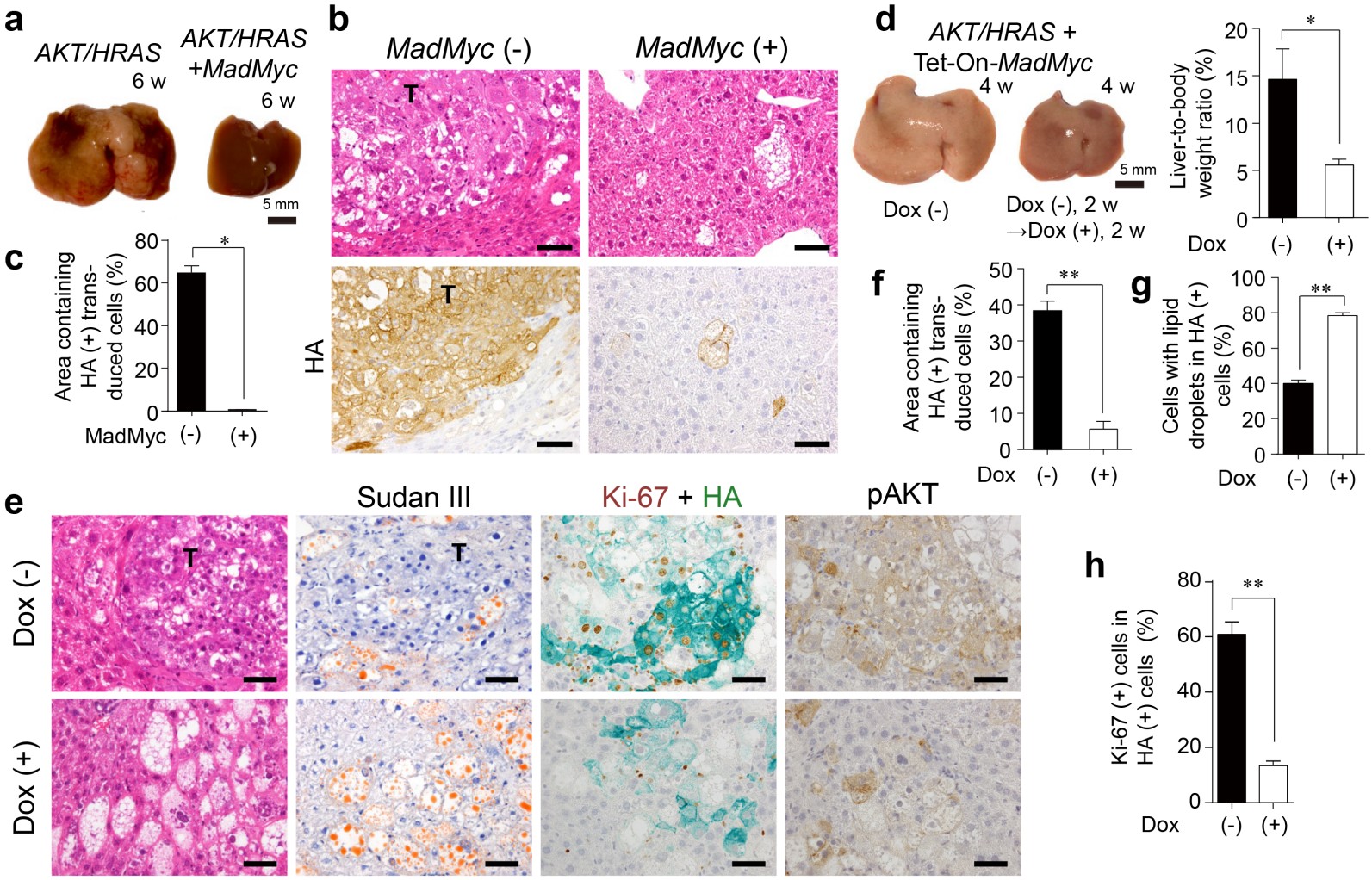

Fig. 4 (Xin et al.)

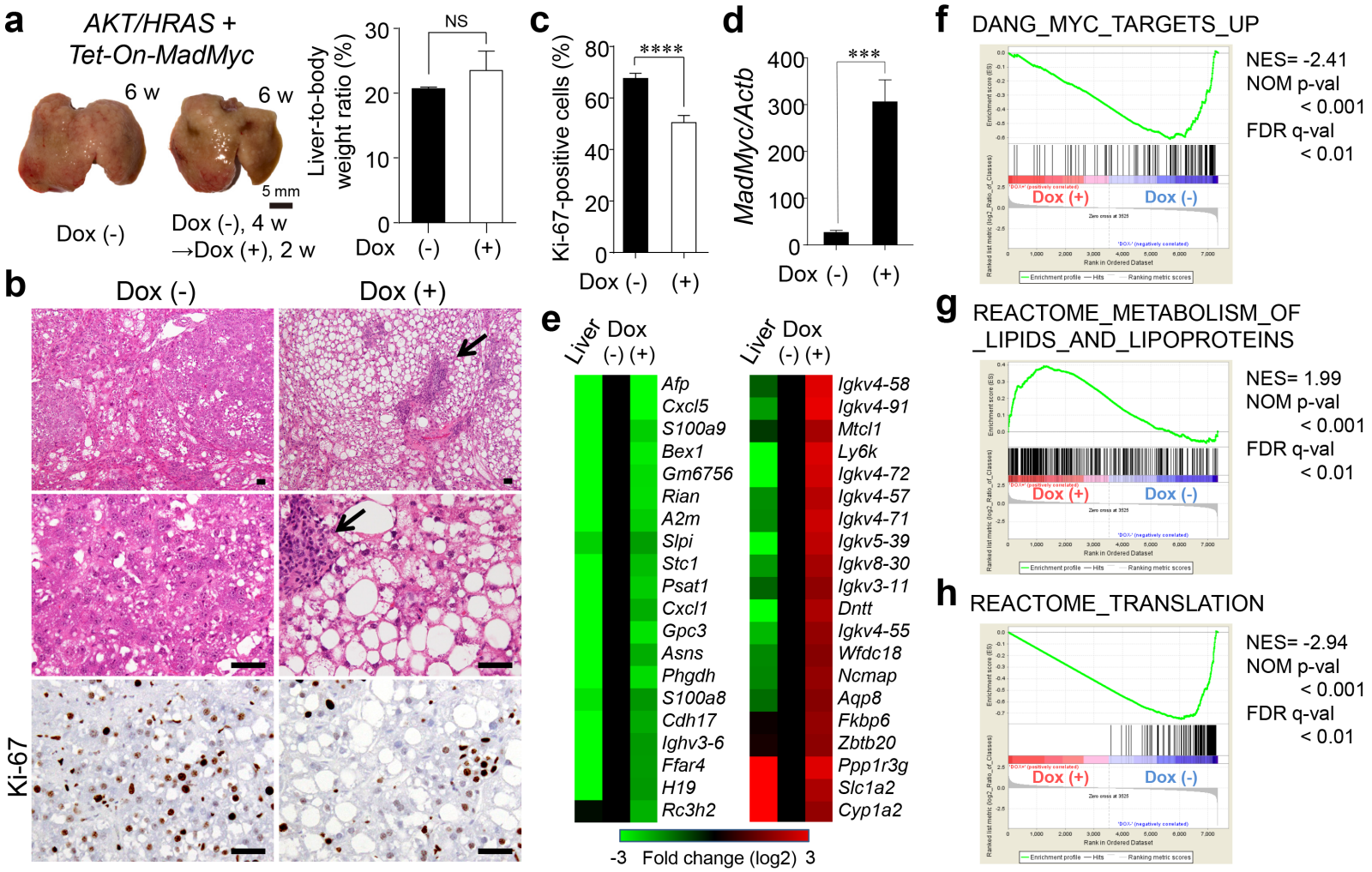

Fig. 5 (Xin et al.)

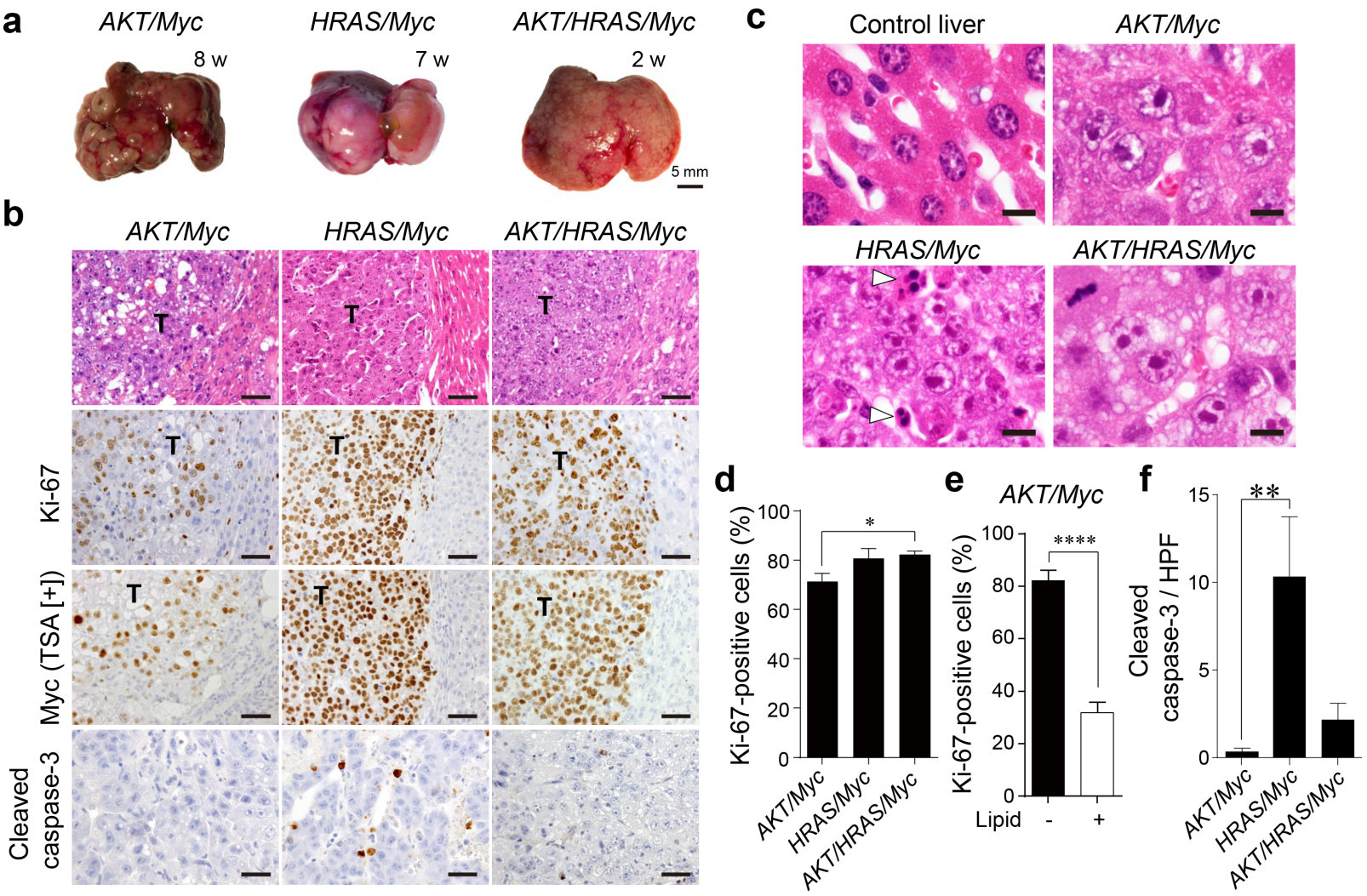

Fig. 6 (Xin et al.)

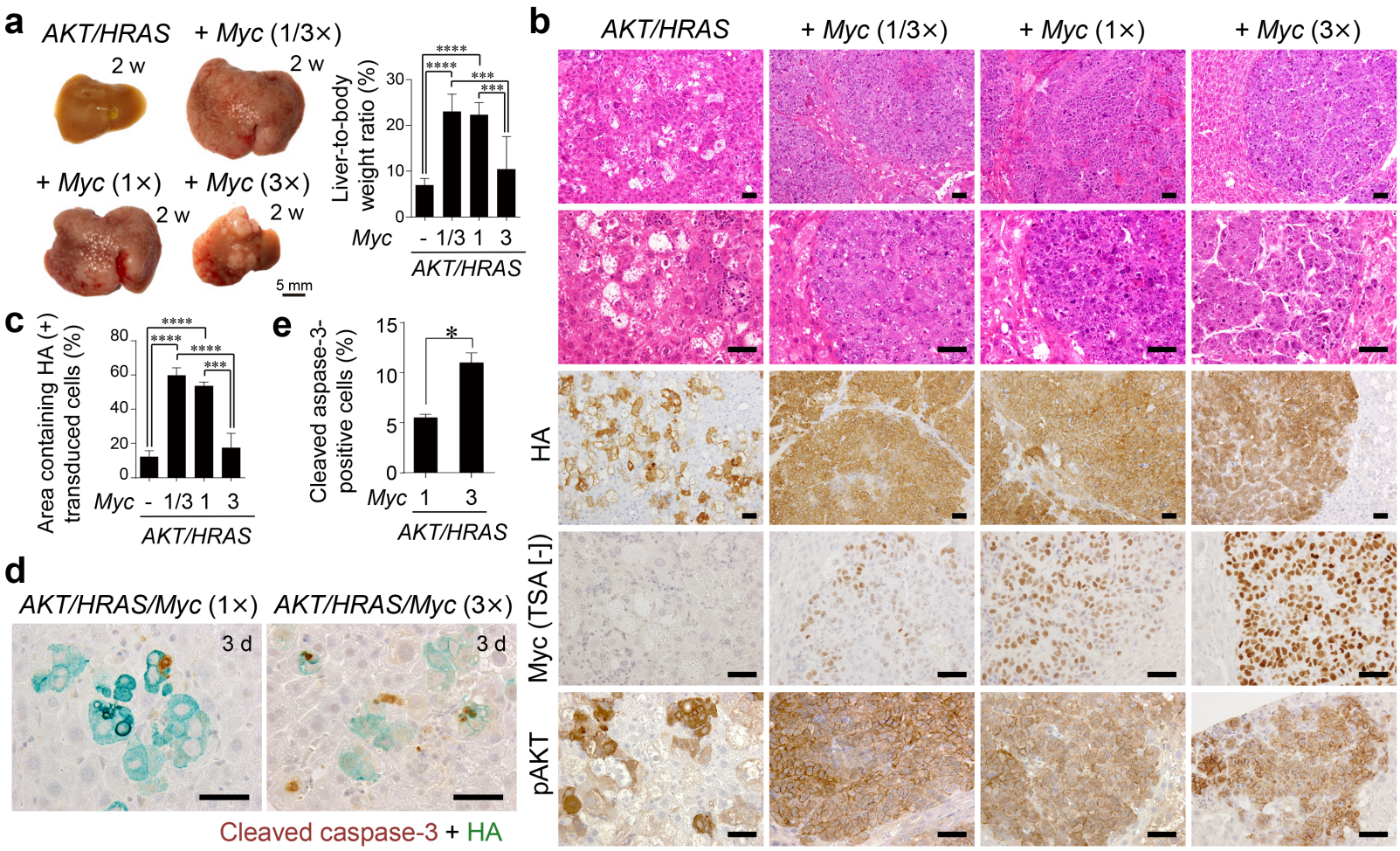

Fig. 7 (Xin et al.)

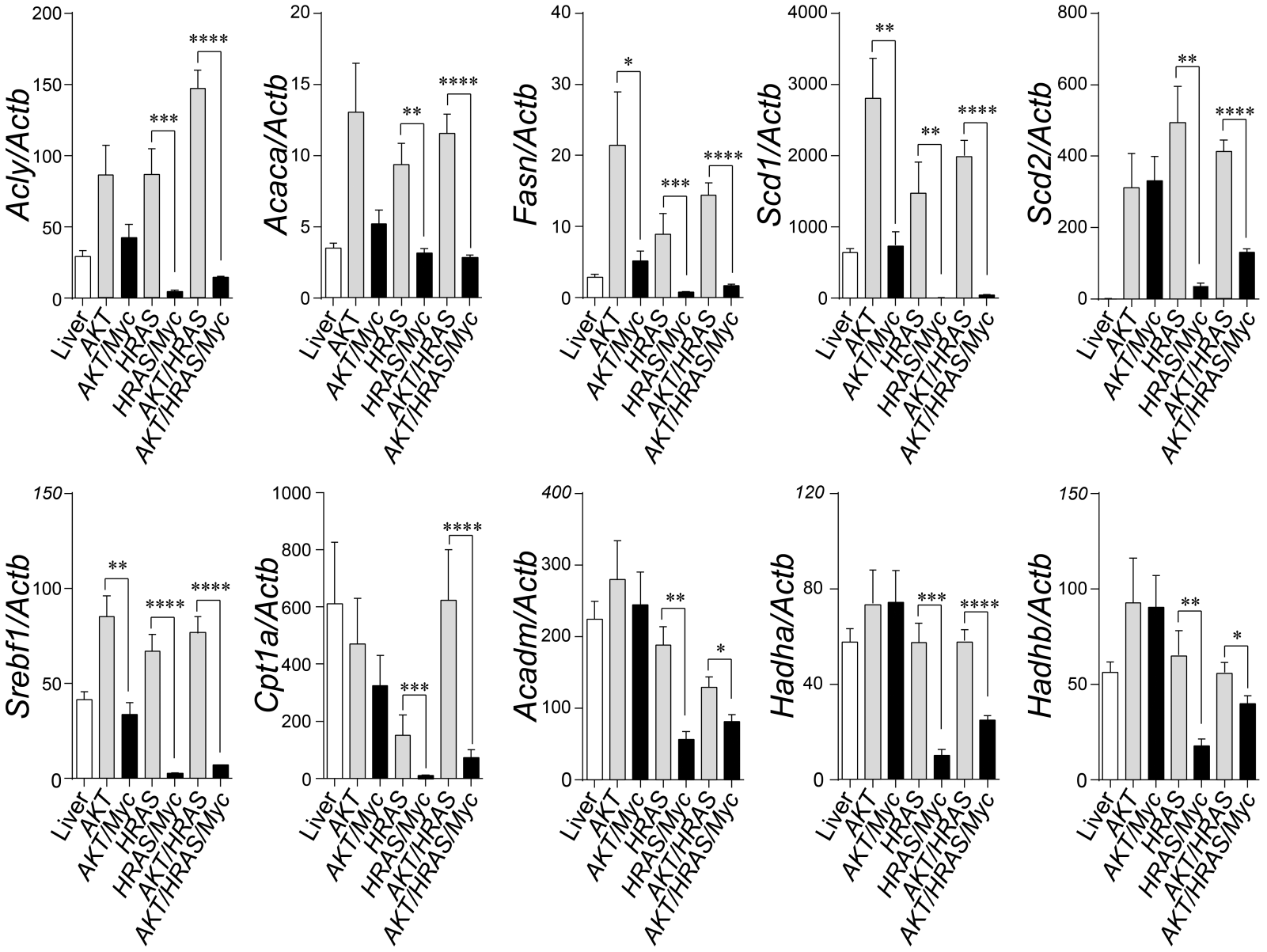

Fig. 8 (Xin et al.)

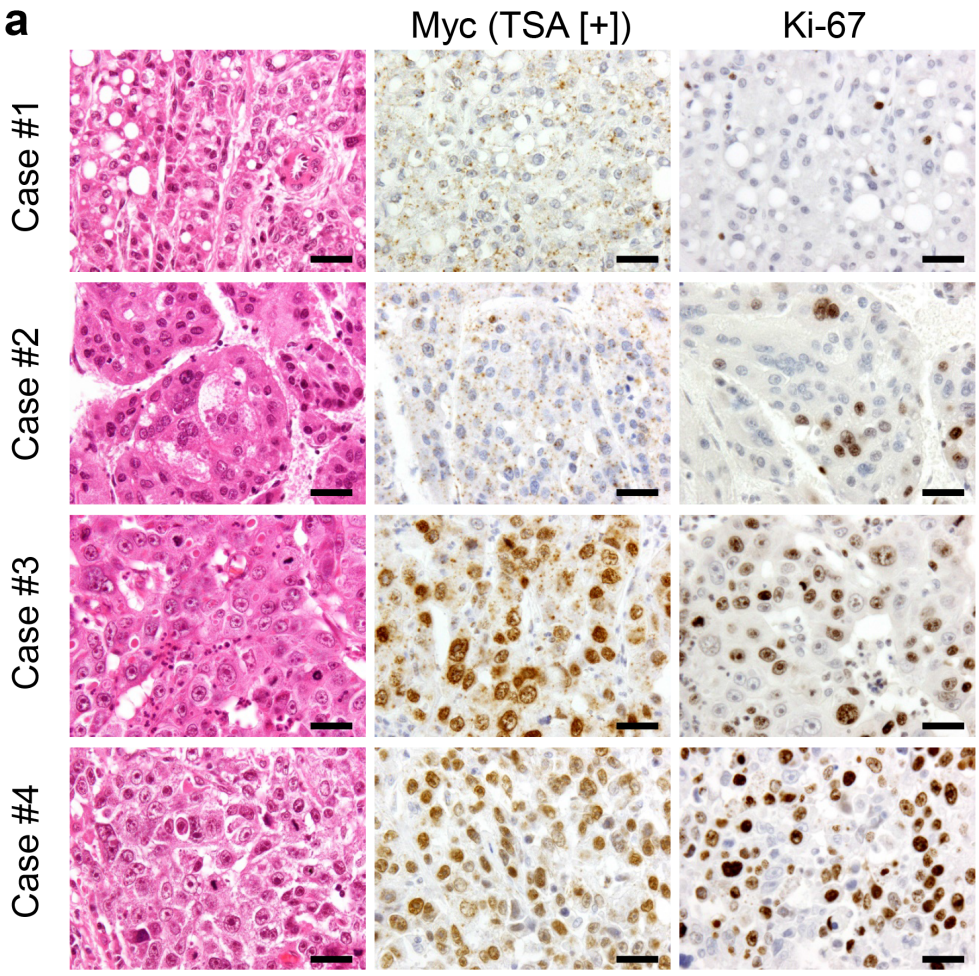

b

		Nuclear Myc expression	
		-	+
Lipid	-	13	9
	+	11	0
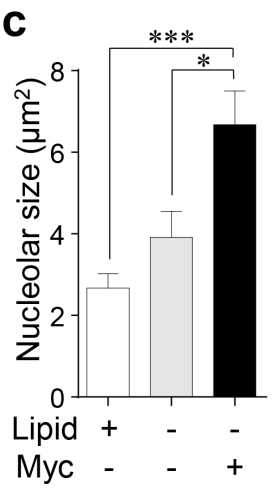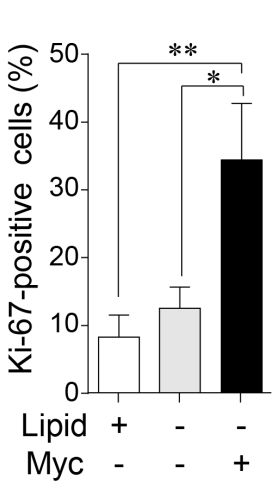
Total number of cases: 33
P = 0.015 (Fisher's exact test)